

HEAT EXCHANGE IN VAPOR CONDENSATION ON TURBULENT  
 JETS OF LIQUID TAKING THE INLET SECTION INTO  
 ACCOUNT

N. S. Mochalova, L. P. Kholpanov,  
 V. A. Malyusov, and N. M. Zhavoronkov

UDC 536.423.4:532.522.2

The article investigates with numerical methods the problem of heat exchange in vapor condensation on turbulent jets of liquid.

Vapor condensation on the surfaces of free jets of cold liquid is distinguished by high intensity of heat exchange; this is of considerable interest for technical applications. However, theoretical calculation of heat exchange has not been sufficiently elaborated, and the available experimental data are also limited.

Under conditions of condensation of pure saturated vapor at pressures that are not too low, the intensity of condensation is determined chiefly by the processes of heat exchange in the jet, which depends on the flow regime, the interphase friction, the geometry of the jet, and on the physical properties of the liquid.

On the basis of the solution of the equations of momentum and energy, the present communication investigates the process of vapor condensation on a turbulent jet of liquid, taking the inlet section into account. It is assumed that the jet of liquid with initial temperature  $T_0$  and velocity distribution over the section of a circular opening with radius  $R_0$ , with  $x = 0$ , flows out into a space filled with saturated vapor of the same liquid, with temperature  $T_s$ , and that the radial component of the temperature gradient is much larger than the axial component. The equations of momentum and energy, describing the process of condensation in turbulent flow of the jet, have the form:

$$u \frac{\partial u}{\partial x} + v \frac{\partial u}{\partial y} = -\frac{1}{\rho} \frac{\partial p}{\partial x} + g + \frac{1}{y} \frac{\partial}{\partial y} \left( \nu_{ef} y \frac{\partial u}{\partial y} \right), \quad (1)$$

$$\frac{\partial(yu)}{\partial x} + \frac{\partial(yv)}{\partial y} = 0, \quad (2)$$

$$u \frac{\partial T}{\partial x} + v \frac{\partial T}{\partial y} = \frac{1}{y} \frac{\partial}{\partial y} \left( a_{ef} y \frac{\partial T}{\partial y} \right), \quad (3)$$

where  $\nu_{ef} = \nu + \nu_T$ ;  $a_{ef} = a + a_T$ . The boundary and initial conditions for the system of equations (1)-(3) are the following:

$$\begin{aligned} &\text{for } x = 0 \quad u = u_0, \quad T = T_0; \\ &\text{for } y = 0 \quad \partial u / \partial y = v = 0, \quad \partial T / \partial y = 0; \\ &\text{for } y = R(x) \quad \partial u / \partial y = \tau_0 / \mu = B, \quad T = T_s. \end{aligned} \quad (4)$$

With the aid of the dimensionless variables

$$\begin{aligned} x &= R_0 \bar{x}; \quad y = R_0 \bar{y}; \quad u = u_0 \bar{u}; \quad v = u_0 \bar{v}; \\ p &= p_0 + \rho u_0^2 \bar{p}; \quad \bar{T} = (T - T_0) / (T_s - T_0) \end{aligned} \quad (5)$$

the system of equations (1)-(3) is transformed, like in [1], to a form suitable for numerical integration

Institute of New Chemical Problems, Moscow. Translated from *Inzhenerno-Fizicheskii Zhurnal*, Vol. 44, No. 6, pp. 902-907, June, 1983. Original article submitted January 27, 1982.

$$u_k \frac{du_k}{dx} = \frac{1}{\text{We}} \frac{1}{R^2(x)} \frac{dR}{dx} + \frac{1}{\text{Re}} \left( \frac{\partial^2 u}{\partial y^2} + \frac{1}{y} \frac{\partial u}{\partial y} \right) + \frac{1}{\text{Fr}} + T_{10}, \quad (6)$$

$$\frac{dy_k}{dx} = A_k \frac{B_N}{1 - A_N} + B_k, \quad (7)$$

$$u_k \frac{dT_k}{dx} = \frac{1}{\text{RePr}} \left( \frac{\partial^2 T}{\partial y^2} + \frac{1}{y} \frac{\partial T}{\partial y} \right) + T_{20}, \quad (8)$$

where

$$T_{10} = \frac{v_T}{R_0 u_0} \left( \frac{\partial^2 u}{\partial y^2} + \frac{1}{y} \frac{\partial u}{\partial y} \right) + \frac{1}{R_0 u_0} \frac{\partial u}{\partial y} \frac{\partial v_T}{\partial y}; \quad (9)$$

$$T_{20} = \frac{a_T}{R_0 u_0} \left( \frac{\partial^2 T}{\partial y^2} + \frac{1}{y} \frac{\partial T}{\partial y} \right) + \frac{1}{R_0 u_0} \frac{\partial T}{\partial y} \frac{\partial a_T}{\partial y}; \quad (10)$$

$$A_1 = B_1 = 0;$$

$$A_{k+1} = \frac{\alpha_{k+1} - u_k}{\alpha_{k+1} + u_{k+1}} A_k - \frac{B_k}{\alpha_{k+1} + u_{k+1}};$$

$$B_{k+1} = \frac{\alpha_{k+1} - u_k}{\alpha_{k+1} + u_{k+1}} B_k - \frac{\Delta_{k+1} + \gamma_{k+1}}{\alpha_{k+1} + u_{k+1}};$$

$$\alpha_{k+1} = \frac{y_k u_k + y_{k+1} u_{k+1}}{y_{k+1} - y_k};$$

$$\beta_{k+1} = \frac{1}{\text{We} R^2} \theta_{k+1}; \quad \gamma_{k+1} = \frac{1}{\text{Fr}} \theta_{k+1};$$

$$\theta_{k+1} = \frac{y_k}{u_k} + \frac{y_{k+1}}{u_{k+1}}; \quad \Delta_{k+1} = \frac{1}{\text{Re}} \left( \frac{y_{k+1}}{u_{k+1}} \Sigma_{k+1} + \frac{y_k}{u_k} \Sigma_k \right);$$

$$\Sigma_{k+1} = \frac{\partial^2 u_{k+1}}{\partial y_{k+1}^2} + \frac{1}{y_{k+1}} \frac{\partial u_{k+1}}{\partial y_{k+1}}.$$

To close the system of equations (6)-(8), two kinds of transfer coefficients were used. One of them is represented by the expression

$$v_T = \text{Pr}_T \varepsilon u(x) R(x), \quad (11)$$

where, according to Kutateladze [2],  $\varepsilon = 5 \cdot 10^{-4}$ , and the value of  $\text{Pr}_T = 0.75$  was taken from the review of experimental works on turbulent heat and mass transfer [3].

The other form of the coefficient of turbulent viscosity was obtained on the basis of Prandtl's theory

$$v_T = \kappa l^2 \left( \frac{\partial u}{\partial y} \right), \quad (12)$$

where  $\kappa = 0.013$  is an experimentally determined constant [4];  $l$  is the mixing length,  $l = \left| \Delta u_m / \left( \frac{\partial u}{\partial y} \right)_m \right|$ ; and  $\Delta u_m$ ,  $(\partial u / \partial y)_m$  are the maximum velocity difference and velocity gradient, respectively.

The system of equations (6)-(8) was integrated numerically by the Runge-Kutta method. As a result of the numerical solution of this system, the velocity and temperature distributions in the cross section and along the jet were found, and with the aid of these dependences the heat-transfer coefficient was determined. To determine the heat-transfer coefficient,  $F$  (2) is multiplied by  $T$ , and (3) by  $y$ , and then the obtained expressions are added together

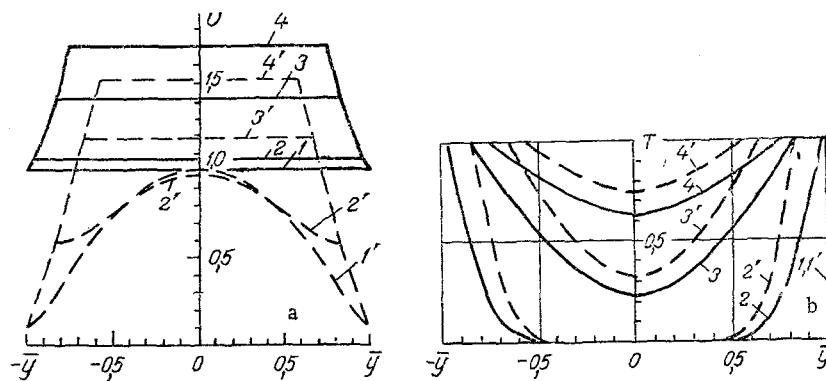


Fig. 1. Change of the velocity profiles (a) and of the temperature profiles (b) along the jet for a plane profile (solid line) and a parabolic profile (dashed line) at the initial section of the jet ( $Re = 2270$ ;  $Pr = 7$ ): 1, 1')  $\bar{x} = 0$ ; 2, 2') 25; 3, 3') 200; 4, 4') 400.

$$\frac{\partial(yuT)}{\partial x} + \frac{\partial(yvT)}{\partial y} = \frac{\partial}{\partial y} \left( a_{ef} y \frac{\partial T}{\partial y} \right).$$

If we integrate the obtained equation with respect to the jet radius, with a view to constant flow rate  $\int_0^R yu dy = \text{const}$ , we obtain the following relation:

$$a_{ef} R \left( \frac{\partial T}{\partial y} \right)_R = \frac{d}{dx} \int_0^R yuT dy, \quad (13)$$

from which follows the expression for the local heat-transfer coefficient

$$\lambda_{ef} \left( \frac{\partial T}{\partial y} \right)_R = \frac{\rho C_p}{R} \frac{d}{dx} \int_0^R yuT dy. \quad (14)$$

The mean heat-transfer coefficient of the surface of the jet is calculated by the formula

$$\alpha = \frac{1}{\Delta T \Pi} \int_0^x 2\pi R(x) \lambda_{ef} \left( \frac{\partial T}{\partial y} \right)_R dx, \quad (15)$$

where  $\Pi$  is the contact surface area of the jet of liquid with the vapor

$$\Pi = \int_0^x 2\pi R(x) dx. \quad (16)$$

With a view to (14), the formula for the mean heat-transfer coefficient is transformed to the following expression:

$$\alpha = \frac{\rho C_p}{\Pi \Delta T} \int_0^x 2\pi \frac{d}{dx} \int_0^R yuT dy dx \quad (17)$$

or

$$\alpha = \rho C_p \mu_0 \frac{\int_0^R yuT dy|_0^x}{\int_0^x R(x) dx}. \quad (18)$$

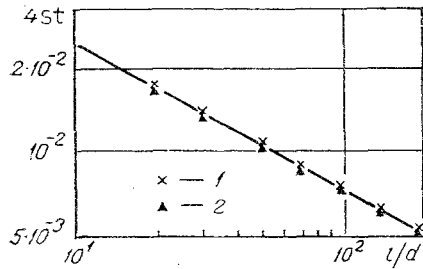


Fig. 2

Fig. 2. Change of the Stanton numbers along the jet for a plane velocity profile at the initial section for  $\epsilon = 5 \cdot 10^{-4}$  and different Weber numbers ( $Re = 1500$ ;  $Pr = 7$ ): 1)  $We = 66$ ; 2) 2500.

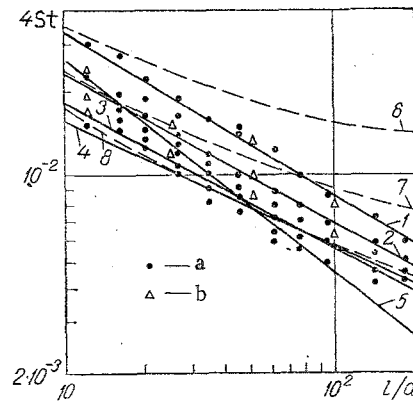


Fig. 3

Fig. 3. Change of the Stanton number along the jet for different ratios of turbulent viscosity and velocity profiles at the initial section:  $v_T = \epsilon Pr u(x) R(x)$ , plane profile: 1)  $\epsilon = 10^{-3}$ ; 2)  $5 \cdot 10^{-4}$ ; 3)  $2.5 \cdot 10^{-4}$ ; profile  $u(0) = 1 - 0.5y^2$ ; 4)  $\epsilon = 5 \cdot 10^{-4}$ ; 5)  $v_T = 0.013L^2 \cdot (du/dy)$ ,  $u(0) = 1 - 0.5y^2$ ,  $\epsilon = 5 \cdot 10^{-4}$ ; calculation by formulas of [5] for different  $\epsilon$ : 6)  $\epsilon = 10^{-3}$ ; 7)  $5 \cdot 10^{-4}$ ; 8)  $2.5 \cdot 10^{-4}$ ; points indicate experimental data: a) of [5]; b) of [6].

We introduce the dimensionless Stanton number

$$St = \alpha / (\rho C_p u_0). \quad (19)$$

If we substitute the expression for the mean heat-transfer coefficient into formula (19), we obtain

$$St = \int_0^R y u T dy \Big|_0^x \int_0^x R(x) dx. \quad (20)$$

When Eqs. (6)-(8) were numerically solved, the Reynolds ( $Re$ ), Froude ( $Fr$ ), Prandtl ( $Pr$ ), and Weber numbers ( $We$ ) changed within the following limits:  $Re$  from 1500 to 20,000,  $Fr$  from 400 to 500,  $Pr$  from 1 to 50, and  $We$  from 50 to 2500.

For studying the range of  $Re$ ,  $Fr$ ,  $Pr$ , and  $We$  numbers it was established that when the numbers  $\bar{B} = BR_0/u_0$  changed from 0 to 0.001, the Stanton number remained practically constant. The small values of  $\bar{B}$  used in the calculations naturally limit the range of application of the obtained results. The results of the calculation may be used, in particular, in cases when interphase friction on the surface of the jet may be neglected.

To shed light on the effect of the initial velocity profile on the heat-transfer coefficient, plane and parabolic velocity profiles were investigated. The development of these velocity profiles is shown in Fig. 1a. The plane profile, specified at the initial section, remains the same at its end. The parabolic profile, specified at the initial section, is transformed into a plane profile. The initial velocity profile has little effect on the shape of the temperature profile but the effect of the velocity at the initial section on the magnitude of the profile is considerable (Fig. 1b).

The Weber number has practically no effect on the Stanton number over the entire extent of change of the length of the jet (Fig. 2).

Figure 3 shows the results of the theoretical calculation by Eqs. (1)-(3), taking into account the expression for turbulent viscosity represented by formulas (11) and (12), and calculation by formulas of [5]; the results of the experimental data of [5, 6] are also plotted.

To determine the mixing length ( $l$ ), the maximum velocity difference and velocity gradient are required. It is understandable that in this case it is incorrect to use the plane velocity profile at the initial section because the maximum velocity difference and velocity gradi-

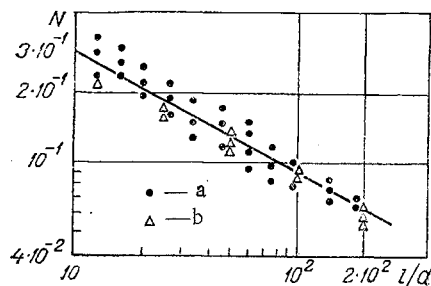


Fig. 4. Dependence of  $N = St / (0.047 \cdot Re^{-0.033} Pr^{0.074} Fr^{-0.064})$  on the dimensionless length of the jet; points indicate experimental data: a) of [5]; b) of [6].

ent will assume zero value everywhere across the thickness of the jet. Therefore, in the initial section a semiparabolic profile was specified to compare the Stanton numbers obtained from different expressions for the coefficient of turbulent viscosity (formulas (11), (12)) by using formula (12).

The semiparabolic profile was used in the calculations solely for the purpose of showing how different formulas for the turbulent transfer coefficient affect the final results of heat exchange.

The results of the present work differ from the hitherto known solutions, e.g., those in [2, 5], by the fact that in the latter works the inlet section was not taken into account. Stipulation of the profile at the initial section affects the slope of the dependence of the Stanton number on the length of the jet. With the same number  $\epsilon = 5 \cdot 10^{-4}$ , the results of calculation by Eqs. (1)-(3) agree better with the experimental data of [5, 6] for the case of specifying a plane profile at the initial section (Fig. 3, curve 2) than for a parabolic profile (Fig. 3, curve 4), and the line 2 approximates the experimental data better over the entire length of the jet. On the basis of this, the results of the solution of Eqs. (1)-(3) for conditions corresponding to curve 2 (Fig. 3) are approximated by the analytical expression of the form

$$St = 0.047 \left( \frac{l}{2R_0} \right)^{-0.52} Re^{-0.033} Pr^{-0.074} Fr^{-0.064} \quad (21)$$

With an accuracy of 10%, formula (21) approximates the theoretical solutions of Eqs. (1)-(3) in the following range of changes of the parameters:  $Re$  from 1500 to 20,000,  $Fr$  from 400 to 5000,  $Pr$  from 1 to 50, and  $We$  from 50 to 2500.

The satisfactory agreement between the theoretical formula (21) and the experimental data of [5, 6] (Fig. 4) makes it possible to recommend this formula for engineering calculations.

#### NOTATION

$x, y$ , orthogonal coordinate system correlated with the axis of symmetry of the jet;  $u, v$ , components of the velocity vector along the coordinates  $x$  and  $y$ ;  $T$ , temperature;  $\nu$ , kinematic viscosity;  $\alpha$ , thermal diffusivity;  $\rho$ , density;  $\lambda$ , thermal conductivity;  $Re = u_0 R_0 / \nu$ , Reynolds number;  $Pr = \nu / \alpha$ , Prandtl number;  $Fr = u_0^2 / (g R_0)$ , Froude number;  $We = (\rho u_0^2 R_0) / \lambda$ , Weber number.

#### LITERATURE CITED

1. N. S. Mochalova, L. P. Kholpanov, V. A. Malyusov, and N. M. Zhavoronkov, "Heat exchange in vapor condensation on a laminar jet of liquid taking the inlet section into account," *Inzh.-Fiz. Zh.*, **40**, No. 4, 581-585 (1981).
2. S. S. Kutateladze, in: *Heat Transfer in Condensation and Boiling* [in Russian], Mashgiz, Moscow (1952), pp. 68-82.
3. L. A. Vulis and V. P. Kashkarov, in: *The Theory of Jets of Viscous Liquid* [in Russian], Nauka, Moscow (1965), pp. 225-227.
4. S. Yu. Krashennnikov, "Calculation of axisymmetric twisted and nontwisted turbulent jets," *Mekh. Zhidk. Gaza*, No. 3, 3-8 (1972).

5. V. P. Isachenko, A. P. Solodov, Yu. Z. Samoilovich, et al., "Investigation of heat exchange in vapor condensation on turbulent jets of liquid," *Teploenergetika*, No. 2, 7-10 (1971).
6. K. V. Demant'eva and A. M. Makarov, "Investigation of vapor condensation on free jets of a cold liquid," in: *Heat and Mass Transfer [in Russian]*, Vol. 11, No. 1, Minsk (1972), pp. 470-474.

EFFECT OF FREE CONVECTIVE HEAT TRANSFER ON THE TEMPERATURE STATE OF SUPERCONDUCTORS

L. L. Guglina, N. T. Bendik,  
L. L. Khlebnikova, and S. K. Smirnov

UDC 536.483

The article investigates the temperature state of a rigid-type coaxial superconductor when the space of the inner core is filled with stagnant helium.

In designing rigid-type coaxial superconductors the problem arises whether it is expedient to evacuate the space of the inner core. In the present work we investigate the additional axial heat influx to the superconducting cores connected with the free convective flow of helium in the space of the inner core, and the effect of this heat influx on the temperature state of the conductor. This investigation is connected with the tests of the experimental section of the superconductor SPK-100 [1], whose diagram of cryostating is shown in Fig. 1. The current-carrying system SPK-100, consisting of two coaxial cores, is made of copper tubes covered with a layer of superconductor  $Nb_3Sn$ . The end sections of the current-carrying system are led into the zone of room temperature, and they form the current lead-ins. The cryoagent helium flows through the coaxial gap, and at the place of contact of the cores with the current lead-ins the flow branches. One part proceeds to cool the current lead-ins, the other returns to the refrigerator. The space of the inner core may be filled with helium at different pressures. The space of the inner core may be filled with helium at different pressures. The heat influx to the cores, which determines the longitudinal temperature distribution, is composed of radial heat influxes through the cryostating shell of the conductor, of heat influxes from the side of the lead-ins due to the thermal conductivity of the metal and the stagnant helium, and also of free convection of the helium. The qualitative temperature distribution along the conductor is shown in Fig. 1. The outer core, far from the current lead-

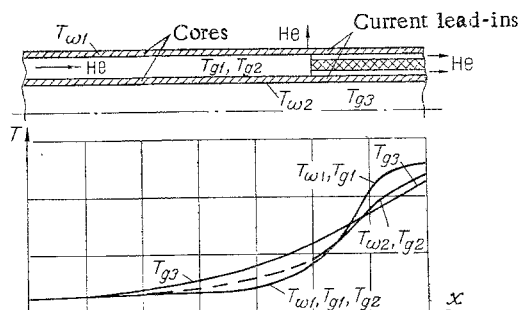


Fig. 1. Diagram of the cryostating of the coaxial conductor and of the temperature distribution: of the outer core  $T_{w1}$ , of the inner core  $T_{w2}$ , of the stagnant helium  $T_{g3}$ , of the cryoagent cooling the CCS  $T_{g1}$ ,  $T_{g2}$  longitudinally.

G. M. Krzhizhanovskii State Research Institute of Power, Moscow. Translated from *Inzhenerno-Fizicheskii Zhurnal*, Vol. 44, No. 6, pp. 907-914, June, 1983. Original article submitted February 22, 1982.